

Article pubs.acs.org/JCTC

# (T)+EOM Ouartic Force Fields for Theoretical Vibrational Spectroscopy of Electronically Excited States

Megan C. Davis and Ryan C. Fortenberry\*



Cite This: J. Chem. Theory Comput. 2021, 17, 4374-4382



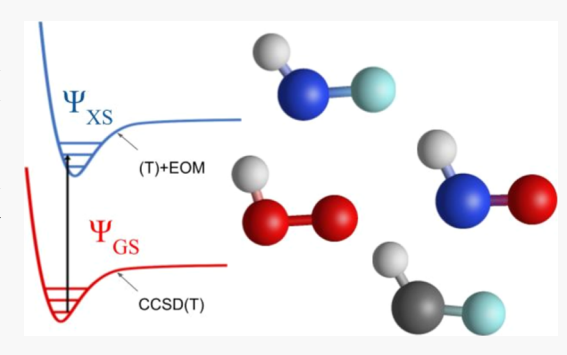
**ACCESS** I

III Metrics & More



Supporting Information

ABSTRACT: (T)+EOM quartic force fields (QFFs) are proposed for ab initio rovibrational properties of electronically excited states of small molecules. The (T)+EOM method is a simple treatment of the potential surface of the excited state using a composite energy from the CCSD(T) energy for the ground-state configuration and the EOM-CCSD excitation energy for the target state. The method is benchmarked with two open-shell species, HOO and HNF, and two closed-shell species, HNO and HCF. A (T)+EOM QFF with a complete basis set extrapolation (C) and corrections for core correlation (cC) and scalar relativity (R), dubbed (T)+EOM/CcCR, achieves a mean absolute error (MAE) as low as 1.6 cm<sup>-1</sup> for the A <sup>2</sup>A' state of HOO versus an established benchmark QFF with CCSD(T)-F12b/ccpVTZ-F12 (F12-TZ) for this variationally accessible electronically excited



state. The MAE for anharmonic frequencies for (T)+EOM/CcCR versus F12-TZ for HNF is 7.5 cm<sup>-1</sup>. The closed-shell species are compared directly with the experiment, where a simpler (T)+EOM QFF using the aug-cc-pVTZ basis set compares more favorably than the more costly (T)+EOM/CcCR, suggesting a possible influence of decreasing accuracy with basis set size. Scans along internal coordinates are also provided which show reasonable modeling of the potential surface by (T)+EOM compared to benchmark QFFs computed for variationally accessible electronic states. The agreement between (T)+EOM/CcCR with F12-TZ and CcCR benchmarks is also shown to be quite accurate for rotational constants and geometries, with an MAE of 0.008 MHz for the rotational constants of (T)+EOM/CcCR versus CcCR for A <sup>2</sup>A' HOO and agreement within 0.003 Å for bond lengths.

## 1. INTRODUCTION

Accurate quantum chemical descriptions of electronically excited states have potential applications for design of optoelectronic devices as well as the detection of interstellar species. 1-3 However, chemical computations are not as well developed for such states when compared with ground-state computations, making quantum chemistry deficient for predicting many necessary properties of molecular systems in higher, bound electronic states.

Coupled cluster theory has achieved remarkable accuracy compared to the experiment, notably with singles, doubles, and perturbative triples, CCSD(T), 4-6 although the triples correction of this method is non-variational and does not produce a triples-corrected wavefunction. Coupled cluster theory may be extended to treat excited states with the equation-of-motion formalism (EOM), which offers a practical and accurate black-box approach. EOM-CCSD is one of the most ubiquitous methods for describing electronically excited states with wavefunction theories, but the lack of triples correlation in EOM-CCSD leads to deficient characterization of singly excited determinants and large inaccuracies for double or higher excitations.8

Multi-configurational methods such as MRCI represent another possible approach, but their dependence on user choice of configurations leaves EOM-based methods as a preferable option in many applications.<sup>2</sup> Time-dependent density functional theory (TD-DFT) is also popular for excited states of large molecules, but the various flavors of O(N<sup>4</sup>) DFT methods lack in accuracy for many applications further depending heavily on intelligent choice of the functional.9,10

Several theories now exist which account for perturbative triples for electronically excited states. 11-15 However, these are not widely available for open shell species, which represent a large portion of electronically excited states of interest. 16 EOM-CC3, an iterative approximate triples method, is available for open-shell systems. 17,18 However, the scaling of this method is generally prohibitive. CR-EOM-CCSD(T) and EOM-CCSD(T) are other approximate triples methods available for open-shell systems, but these methods correct the excitation energy while still using a CCSD reference state,

Received: March 29, 2021 Published: June 24, 2021





which can hinder achieving desired accuracy for the total energy. <sup>19,20</sup>

A major application for quantum chemistry is the calculation of theoretical vibrational and rotational frequencies, which may be used to help detect interstellar molecules among other applications. 3,21 This has been successfully done using quartic force fields (QFFs) to accuracy within 5 cm<sup>-1</sup> of experiment for vibrational modes and 30 MHz for rotational constants. 21-33 Theoretical calculation of these frequencies using OFFs for electronically excited states could help in the detection of more species via rovibronic spectroscopy or even direct detection of highly populated electronic states. Electronically excited states are often treated variationally with these ground state-type methods. This has been done in the past with molecules such as H<sub>2</sub>SS<sup>+,34</sup> Such an approach is limited to vibrational modes that preserve the symmetry of the molecule, making the excited states variationally accessible and is likely to fail or potentially not even be able to treat states with higher than singly excited determinants.

QFFs have previously been extended to treat electronically excited states through the usage of EOM-CC3. <sup>26,35</sup> However, these attempts have not resulted in sufficient accuracy and the computational scaling of EOM-CC3 is prohibitive for relatively modest species. The present work attempts to formulate a simple yet versatile methodology for treating electronically excited states with highly accurate QFFs. This method calculates ground-state energies and excitation energies separately using CCSD(T) and EOM-CCSD, respectively, utilizing the same geometry and even reference CCSD wavefunction. The implication is that such an approach sidesteps the issue of EOM not being applicable to CCSD(T) and provides a large deal of flexibility because these computational methods are widely available in quantum chemistry packages for both closed and open-shell systems.

## 2. METHODS

A QFF is a fourth-order Taylor series expansion of the internuclear potential portion of the Watson Hamiltonian (eq 1), which may be used with second-order vibrational perturbation theory (VPT2) to generate spectroscopic data.

$$V = \frac{1}{2} \sum_{ij} F_{ij} \Delta_i \Delta_j + \frac{1}{6} \sum_{ijk} F_{ij} \Delta_i \Delta_j \Delta_k + \frac{1}{24} \sum_{ijkl} F_{ij} \Delta_i \Delta_j \Delta_k \Delta_l$$
(1)

For computing a QFF, the geometry is first tightly optimized at a given level of theory to obtain a reference geometry. Displacements from this reference geometry are then made along the molecule's symmetry internal coordinates using step sizes of 0.005 Å or 0.005 radians. The single-point energy at the desired level of theory is calculated at each of these displacements. The relative energies are then refitted to the exact minimum and used to generate force constants using a least squares fitting procedure. The force constants are transformed from symmetry internal to Cartesian coordinates using INTDER.<sup>36</sup> The Cartesian force constants are then fed into SPECTRO,<sup>37</sup> which uses second-order vibrational perturbation theory (VPT2) to generate fundamental vibrational frequencies and rotational constants as well as other spectroscopic data of interest.<sup>38–40</sup>

Two ground-state QFFs are used as benchmarks. The first is based entirely on the CCSD(T)-F12b energy $^{41}$  with the ccpVTZ-F12 basis set $^{42-44}$  and will be referred to as F12-TZ

from here on. The second quartic force field is constructed by using a composite reference geometry which consists of a CCSD(T)/aug-cc-pV5Z geometry with corrections for core correlation at the CCSD(T) level using the Martin-Taylor core-correlating basis set. The single-point energies are then calculated using a three-point complete basis set extrapolation using aug-cc-pVXZ (X = T,Q,5) basis sets with additive corrections for core correlation again using the Martin-Taylor basis set and scalar relativity using the Douglass-Kroll formalism. This is dubbed the CcCR method. This composite method could be made more accurate with the inclusion of higher-order correlation, but this has been shown to have a negligible effect on spectroscopic accuracy, leaving CcCR as a reliable high-level benchmark. All computations for both of these QFFs are done using MOLPRO 2015.

The methodology proposed in this paper for treating electronically excited states is dubbed the (T)+EOM method. Energies are obtained using a composite of the CCSD(T) ground-state energy plus the excitation energy to the target state at the EOM-CCSD level of theory, with both terms using the same basis set (e.g., aug-cc-pVTZ) at the same geometry

$$E_{(T)+EOM/avtz}^{xs} = E_{CCSD(T)/aug-cc-pVTZ}^{gs} + E_{EOM-CCSD/aug-cc-pVTZ}^{xs}$$
(2)

Optimized reference geometries for the target state are obtained by numerically optimizing the composite (T)+EOM energy. Thus, the QFF can be constructed using (T)+EOM reference geometry and single-point energies in a straightforward manner in a similar process as the ground-state-type QFFs.

Two (T)+EOM-based QFFs are utilized in this paper. The (T)+EOM/avtz quartic force field is constructed using (T)+EOM energies with an aug-cc-pVTZ basis set, as shown in eq 2. The other is modeled after the CcCR QFF but with the additional EOM portion included and is called (T)+EOM/CcCR. The reference geometry for this QFF is obtained by compositing the optimized geometry at the (T)+EOM/aug-cc-pV5Z level with (T)+EOM/Martin-Taylor corrections

$$R_{(T)+EOM/CcCR} = R_{(T)+EOM/aug-cc-pV5Z} + (R_{(T)+EOM/MTcore} - R_{(T)+EOM/MT})$$
(3)

The single-point energies are calculated, similarly to the ground-state CcCR QFF, by compositing a TQ5 complete basis set extrapolation with core correlation and scalar relativistic corrections, using the Martin-Taylor basis set and Douglas-Kroll formalism, respectively. Effectively, this represents a doubling of the number of computations necessary for a single point, one set with CCSD(T) and the other with EOM-CCSD. The combination of the two approaches is implied from here on. The total energy for the (T)+EOM/CcCR approach is given below

$$\begin{split} E_{\text{(T)+EOM/CcCR}} &= E_{\text{(T)+EOM/CBS}} + (E_{\text{(T)+EOM/MTcore}} \\ &- E_{\text{(T)+EOM/MT}}) \\ &+ (E_{\text{(T)+EOM/DKrel}} - E_{\text{(T)+EOM/DK}}) \end{split} \tag{4}$$

Four triatomic molecules with low-lying excited states are chosen as test cases for the (T)+EOM method. Two of these

Table 1. Ã <sup>2</sup>A' HOO Harmonic and Anharmonic Vibrational Frequencies

	$\omega_1$	$\omega_2$	$\omega_3$	$ u_1$	$ u_2$	$ u_3$
description	H-O str.	H-O-O bend	H-O str.	H-O str.	H-O-O bend	H-O str.
F12-TZ	3742.7	1233.4	962.4	3552.4	1193.7	937.6
CcCR	3749.5	1235.7	966.2	3555.6	1164.3	935.6
CCSD(T)/av5z <sup>a</sup>	3744.3 (3744.3)	1232.8 (1232.8)	961.3 (961.4)	3554.8 (3553.3)	1194.3 (1167.9)	937.4 (932.6)
(T)+EOM/avtz	3720.2	1225.2	938.6	3534.2	1187.7	915.7
(T)+EOM/CcCR	3742.3	1236.6	962.4	3549.1	1195.1	937.9
CC3/avtz	3723.2	1220.3	949.9	3538.6	1182.3	926.1
CC3/avqz	3740.5	1226.3	963.4	3550.7	1187.9	938.8
CC3/avqz + MTc	3746.3	1227.4	965.6	3555.3	1189.0	940.6
$experiment^b$				3268.5	1285	929.068

"QFF with single-point energies calculated in PSI4. Results using MOLPRO in parenthesis. bFink, Kruse, et al. (gas phase);  $\nu_3$ : Hunziker and Wendt, 1976 (gas phase); Becker, Fink, et al., 1978 (gas phase); Holstein, Fink, et al., 1983 (gas phase). 52-55

are radicals in their ground-state configuration:  $\tilde{X}^2A''$  HOO and  $\tilde{X}^2A''$  HNF. The other two are closed shell species:  $\tilde{X}^1A'$  HCF, and  $\tilde{X}^1A'$  HNO. These molecules have a relatively small number of electrons, and therefore, high levels of theory are not prohibitively expensive to use for benchmarking. These molecules are selected to cover several different types of bonds of common interstellar species (N, C, and O) and also based on the availability of experimental data for the electronically excited states.

The excited states of the radical species are treated with the F12-TZ and CcCRQFFs for both configurations since the higher states are variationally accessible in order to provide benchmarks for the excited state QFFs based on pure theoryto-theory comparison. The EOM description of the A states of HOO and HNF are both also dominated by a single determinant, so these benchmarks should be reliable. The excited state configurations are treated with (T)+EOM/avtz and (T)+EOM/CcCR.  $\bar{A}^2A'$  HOO is also treated withEOM-CC3/aug-cc-pVTZ and EOM-CC3/aug-cc-pVQZ both with and without Martin Taylor core correlation. The singlet species are only treated with (T)+EOM/avtz and(T)+EOM/ CcCR, because MOLPRO 2015 is not equipped to handle the singlet biradical excited state configurations of these molecules. NWChem<sup>50</sup> is used for the (T)+EOM calculations for all doublet species because of its support for open-shell EOM-CCSD. However, the excited states of the singlet species are treated with (T)+EOM in MOLPRO for performance reasons, because (T)+EOM only requires closed-shell EOM-CCSD for these species.

All four molecules are of the H–A–B pattern and follow the same simple internal coordinate scheme for displacements in the QFF procedure. This consists of the H–A stretch, the A–B stretch, and the H–A–B bend, resulting in 129 total displacements to form the complete QFF. Fermi resonances and their polyads are also taken into account by SPECTRO. The resonances are a  $2\nu_2 = \nu_1$  type-1 Fermi resonance for  $\tilde{A}^1A''$  HNO; a  $2\nu_3 = \nu_2 + \nu_3 = \nu_1$  polyad for  $\tilde{X}^1A'$  HNO; and a  $2\nu_2 = \nu_2 + \nu_3 = \nu_1$  polyad for  $\tilde{X}^1A'$  HCF.

Adiabatic excitation energies (AEE) for (T)+EOM/CcCR are calculated by subtracting the difference between the (T)+EOM/CcCR energy of the electronically excited state at the optimized geometry from the CcCR ground-state energy at the optimized CcCR geometry. Each energy term also includes fitting corrections and anharmonic zero-point energy (ZPE) corrections from the QFF procedure. A similar process is used for CcCR AEEs using CcCR energies of the variationally accessible excited state in place of (T)+EOM/CcCR energies.

### 3. RESULTS AND DISCUSSION

3.1. HOO. (T)+EOM/CcCR compares extremely well with the F12-TZ benchmark QFF for the  $\tilde{A}^2A'$  state of HOO, with a mean absolute error (MAE) of 1.6 cm<sup>-1</sup> between the anharmonic frequencies given in Table 1. The comparison is slightly less favorable with CcCR due to the  $\nu_2$  mode, which at 1164.3 is 29.4 cm<sup>-1</sup> lower than the F12-TZ at 1193.7 cm<sup>-1</sup>. All CC3 calculations given are, however, in much closer agreement with F12-TZ than with CcCR. This suggests a possible error in the CcCR's handling of the  $\nu_2$  mode. Data from quartic force fields based on CCSD(T)/aug-cc-pV5Z energies run in both MOLPRO and PSI4 show PSI4 agreeing with other methods and placing  $\nu_2$  at 1994.3 cm<sup>-1</sup>. MOLPRO places it 26.4 cm<sup>-1</sup> lower. The discrepancy here and in CcCR is, thus, potentially due to an inconsistency in MOLPRO's RHF-UCCSD(T) code, as further investigation reveals MOLPRO assigning an illogical orbital energy of -0.7555 Hartree to the singly occupied molecular orbital compared to -0.2555 Hartree for PSI4 despite agreeing with PSI4 in the total ROHF energy. In any case, the cheaper (T)+EOM/avtz QFF also agrees reasonably well with F12-TZ with an MAE of 15.4 cm<sup>-1</sup>.

Comparison with available experimental data is somewhat less favorable. Modes  $\nu_1$  and  $\nu_2$  do not compare well between the theory and experiment, with a difference of 283.9 and 91.3 cm $^{-1}$ , respectively, for the F12-TZ versus experiment. Calculated AEEs match well with the available experimental excitation energy for this state of 7030 cm $^{-1}$ ,  $^{52-54}$  with an AEE for CcCR at 6983 cm $^{-1}$  using a ground-state treatment of the variationally accessible excited state. The AEE for (T)+EOM/CcCR is 6878 cm $^{-1}$  agrees moderately well with a difference of 151 cm $^{-1}$  below the experiment. Additionally, CC3 and (T)+EOM calculations both agree much more closely with F12-TZ and CcCR than with the experiment. This suggests either a possible misassignment of these experimental frequencies or a systematic flaw in a coupled cluster-based approach to these modes.

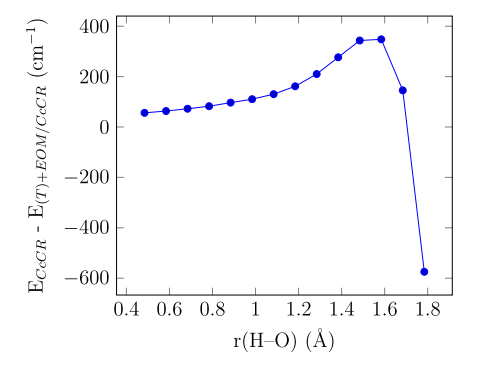
Computed frequencies for the  $\tilde{X}^2A''$  state of HOO are given in Table S1; geometries are given in Table S2. Good agreement is shown here between F12-TZ and CcCR, which vary by no more than 6 cm<sup>-1</sup> for anharmonic frequencies. These values agree closely with the available experiment for the  $\nu_2$  and  $\nu_3$  modes. However  $\nu_1$ , which corresponds with the H–O stretch, is about 35 cm<sup>-1</sup> lower for the experiment compared to CcCR. A possible explanation is that the description of this H–O stretching mode may be deficient for coupled-cluster-based QFFs in general, regardless of the electronic state.

Table 2.  $\tilde{A}$  <sup>2</sup>A' HOO Geometry and Rotational Frequencies

					T+EOM		CC3		
	units	F12-TZ	CcCR	avtz	CcCR	avtz	avqz	avqz + MTc	
$R_0(H-O)$	Å	0.981	0.979	0.983	0.980	0.983	0.981	0.980	
$R_0(O-O)$	Å	1.403	1.400	1.416	1.402	1.413	1.405	1.402	
∠0(H-O-O)	deg	102.015	102.114	101.618	102.109	101.772	102.113	102.242	
$A_0$	MHz	20.191	20.273	19.988	20.252	20.027	20.199	20.261	
$B_0$	MHz	1.021	1.026	1.003	1.023	1.007	1.019	1.022	
$C_0$	MHz	0.969	0.973	0.952	0.970	0.956	0.967	0.970	
$A_1$	MHz	19.361	19.436	19.184	19.420	19.217	19.370	19.428	
$B_1$	MHz	1.021	1.026	1.003	1.023	1.007	1.019	1.022	
$C_1$	MHz	0.967	0.971	0.950	0.969	0.954	0.965	0.968	
$A_2$	MHz	20.892	20.977	20.676	20.954	20.723	20.906	20.973	
$B_2$	MHz	1.022	1.027	1.004	1.024	1.008	1.020	1.023	
$C_2$	MHz	0.966	0.970	0.949	0.967	0.953	0.964	0.967	
$A_3$	MHz	20.233	20.316	20.019	20.295	20.063	20.242	20.306	
$B_3$	MHz	1.009	1.013	0.991	1.011	0.995	1.007	1.010	
$C_3$	MHz	0.956	0.960	0.940	0.958	0.943	0.954	0.957	

Table 2 compares vibrationally averaged geometric parameters and rotational frequencies (where  $A_0$ ,  $A_1$ ...are the rotational constants corresponding to each vibrational level) for the  $\tilde{A}^{2}A'$  state of HOO. A good agreement is shown between geometric parameters. The  $r_0(H-O)$  bond length agrees to within 0.003 Å for all methods.  $r_0(O-O)$  agrees similarly well, although (T)+EOM/avtz and CC3/avtz are off by about 0.010 Å. This is likely due to the small basis set sizes, as (T)+EOM/CcCR and CC3/avqz fall in line with the benchmark parameters. A similar circumstance is produced with  $\angle$ (H-O-O), where (T)+EOM/CcCR agrees with CcCR to within 0.01°. The rotational constants also compare quite well, with an MAE of 0.008 MHz for (T)+EOM/CcCR versus CcCR. (T)+EOM/CcCR, and to a lesser extent (T)+EOM/avtz, appears to approximate the accurate ground-state-type quartic force fields reasonably based on this test case.

A scan along the H–O bond length for  $\tilde{A}$   $^2A'$  HOO was performed in order to investigate the agreement between CcCR and (T)+EOM/CcCR in the description of the excited state surface. Figure 1 shows the difference, in cm<sup>-1</sup>, between (T)+EOM/CcCR and CcCR energies from bond lengths 0.48422 to 2.18422 Å at step sizes of 0.1 Å. This is a constrained scan using the CcCR geometry as a reference point. This shows very close agreement between the two methods near the equilibrium point. The agreement starts to



**Figure 1.** Constrained r(H-O) scan for  $\tilde{A}^{2}A'$  HOO comparing (T)+EOM/CcCR  $\nu s$  variationally accessible CcCR. Equilibrium bond distance is 0.96844 Å.

break down at further bond distances. The equilibrium H–O bond length for CcCR is 0.96844 Å. The difference between (T)+EOM/CcCR and CcCR near this length is 110.4 cm<sup>-1</sup> at 0.98422 Å. The agreement is closer at smaller values of H–O, though this is likely due to the nuclear repulsion term dominating, minimizing the difference between methods. (T)+EOM/CcCR maintains reasonable accuracy until the bond length approaches 1.8 Å, where the values diverge. However, the QFF only uses step sizes of 0.005 Å or radians so this implies that the portion of the potential surface near the minimum is being sufficiently modeled by (T)+EOM/CcCR.

Additional similar scans are also performed for HOO. Table S1 shows comparison between (T)+EOM/CcCR and CcCR. Tables S2-S4 show comparison between (T)+EOM/avtz and CCSD(T)/avtz for all three degrees of freedom. The data from these scans follow similar trends to Figure 1, where the given (T)+EOM method approximates the analogous ground-state-type energies near the minimum.

**3.2. HNF.** Table 3 shows vibrational frequencies for  $\tilde{A}^2A'$ HNF, the other open shell reference molecule studied. CcCR and F12-TZ agree much more closely here, showing none of the disagreement seen in the  $\nu_2$  mode of  $\tilde{A}^2A'$  HOO.  $\nu_3$ compares well with the gas-phase measurements of Woodman,<sup>56</sup> with only a 0.7 cm<sup>-1</sup> difference from the F12-TZ and a 4.9 cm<sup>-1</sup> variance from the CcCR. Agreement between the two benchmark methods and Woodman's measurement for  $\nu_2$  is not as high, with Woodman placing this mode at 1121 cm<sup>-1</sup> compared to 1142.3 cm<sup>-1</sup> for CcCR, and the  $\nu_3$  mode for all methods disagrees with the results of Jacox and Milligan. 57 The results of the latter are from Argon matrix data and are likely to be red-shifted, which could explain the discrepancy. Additionally, the agreement between benchmark methods and experiment is expected to differ between 6 and 30 cm<sup>-1</sup> of the experiment. CcCR often shows errors which are attributable to the composite nature of the method. 26,58,59 F12-TZ, while generally more consistent due to being based on a single energy term, still displays these discrepancies even for very similar molecules.60-

(T)+EOM/CcCR again compares exceptionally well with the benchmark QFFs with an MAE of 7.5 cm<sup>-1</sup> versus F12-TZ and 10.4 cm<sup>-1</sup> versus CcCR. (T)+EOM/CcCR makes a significant improvement over the less robust (T)+EOM/avtz QFF in the  $\nu_1$  and  $\nu_2$  modes, with (T)+EOM/avtz 11.3 cm<sup>-1</sup>

Table 3. Ã <sup>2</sup>A' HNF Harmonic and Anharmonic Vibrational Frequencies

HNF A'	$\omega_1$	$\omega_2$	$\omega_3$	$ u_1$	$ u_2$	$ u_3$
description	H-N str.	N-F str.	H-N-F bend	H-N str.	N-F str.	H-N-F bend
F12-TZ	3526.0	1167.0	1113.1	3339.9	1138.7	1074.7
CcCR	3535.1	1170.9	1113.5	3348.1	1142.3	1078.9
(T)+EOM/avtz	3505.5	1149.5	1101.3	3319.9	1122.3	1068.5
(T)+EOM/CcCR	3523.0	1172.7	1112.8	3331.2	1144.3	1066.7
Exp.a					1121	1074
Exp. <sup>b</sup>						1033
<sup>a</sup> Woodman, 1970 (gas pl	nase). <sup>56</sup> <sup>b</sup> Jacox and	Milligan, 1967 (	Argon). <sup>57</sup>			

lower for  $\nu_1$  and 22.0 cm<sup>-1</sup> lower for  $\nu_2$ . This suggests that the TQ5 complete basis set extrapolation as well as the additive corrections are important for (T)+EOM QFFs to achieve desirable accuracy. (T)+EOM/avtz actually produces the closest agreement with Woodman with only a 1.3 cm<sup>-1</sup> difference between the two. However, this may be coincidental. Jacox and Milligan place the  $\tilde{A}^2A' \leftarrow X^2A''$  excitation energy at 20,140 cm<sup>-1.57</sup> The calculated AEE for (T)+EOM/CcCR is

Table 4 contains the geometric parameters and rotational constants for  $\tilde{A}$   $^2A'$  HNF. A good agreement is seen between

20,149 cm<sup>-1</sup>, a difference of less than 10 cm<sup>-1</sup>!

Table 4. Ã <sup>2</sup>A' HNF Geometry and Rotational Frequencies

				(T)+	EOM
	units	F12-TZ	CcCR	avtz	CcCR
$R_0(H-N)$	Å	1.027	1.025	1.029	1.026
$R_0(N-F)$	Å	1.344	1.341	1.351	1.340
$\angle 0(H-N-F)$	Å	122.846	122.984	122.929	123.167
$A_0$	MHz	27.226	27.417	27.148	27.512
$B_0$	MHz	1.035	1.038	1.024	1.039
$C_0$	MHz	0.993	0.996	0.983	0.997
$A_1$	MHz	25.945	26.131	25.868	26.220
$B_1$	MHz	1.032	1.035	1.021	1.036
$C_1$	MHz	0.989	0.992	0.978	0.993
$A_2$	MHz	27.318	27.504	27.421	27.678
$B_2$	MHz	1.025	1.028	1.014	1.029
$C_2$	MHz	0.986	0.989	0.977	0.990
$A_3$	MHz	29.373	29.616	29.127	29.667
$B_3$	MHz	1.035	1.038	1.023	1.039
C <sub>3</sub>	MHz	0.986	0.989	0.975	0.990

(T)+EOM/CcCR, CcCR, and F12 for  $r_0(H-O)$  and  $r_0(O-O)$ , with (T)+EOM/avtz having a slightly higher value than the others at 1.351 Å for O-O *versus* 1.341 Å for CcCR. The  $\angle(H-O-O)$  is slightly higher for (T)+EOM/CcCR *versus* the benchmarks, at 123.167° compared to 122.984° for CcCR.

This may be responsible for the  $\nu_3$  mode shifting 1.8 cm<sup>-1</sup> away from the benchmarks for (T)+EOM/CcCR compared to (T)+EOM/avtz. Rotational constants for (T)+EOM/CcCR, again, agrees well with F12-TZ and CcCR with an MAE of 0.035 MHz *versus* CcCR.

The vibrational frequencies for the  $\tilde{X}$   $^2A''$  state of HNF are given in Table S4. The rotational constants and geometric parameters are given in Table S5. These produce similar values between F12-TZ and CcCR. Both of which compare quite well with the experiment. Scans are given for the H-N bond length (Figure S5), N-F bond length (Figure S6), and H-N-F bond angle (Figure S7). These scans show an excellent agreement between (T)+EOM/avtz and CCSD(T)/avtz around the optimized minimum for CCSD(T)/avtz for the  $\tilde{A}$   $^2A'$  state, again suggesting that (T)+EOM reasonably models the potential energy surface of the electronically excited state.

**3.3. HCF and HNO.** The (T)+EOM QFFs for the  $\tilde{A}^{-1}A''$ states of HCF and HNO are compared directly to available experimental data. Table 5 shows the vibrational frequencies for  $\tilde{A}$   $^{1}A''$  HCF. The agreement is reasonable between (T)+EOM/avtz and the gas phase data of Nauta, et al.<sup>63</sup> for  $\nu_1$ , with a difference of 2.9 cm<sup>-1</sup> between the two. The (T)+EOM/CcCR value for this mode is slightly higher, at 2813.3 cm<sup>-1</sup> compared to 2799.7 cm<sup>-1</sup>. A similar trend is seen with the  $\nu_2$  mode, where (T)+EOM/avtz at 1259.3 cm<sup>-1</sup> is quite close to 1260 cm<sup>-1</sup> from the gas phase data of Schmidt et al.64 This closer agreement with the experiment may be coincidental, though it could indicate some advantages of (T)+EOM/avtz compared to (T)+EOM/CcCR. Part of the (T)+EOM energy is the energy of the CCSD(T) ground-state configuration at the (T)+EOM excited state geometry. This may lead to inaccuracies if the excited state geometry is significantly different than the ground-state geometry, as accurate CCSD(T) energies rely on proximity to a minima on the potential surface. This effect may be exacerbated by the larger basis sets used in (T)+EOM/CcCR. The (T)+EOM method may therefore perform better with excited states that

Table 5. Ã <sup>1</sup>A" HCF Harmonic and Anharmonic Vibrational Frequencies

	$\omega_1$	$\omega_2$	$\omega_3$	$ u_1$	$ u_2$	$ u_3$
description	H-C str.	H-C-F bend	C-F str.	H-C. str.	H-C-F bend	C-F str.
(T)+EOM/avtz	2992.0	1286.2	1026.4	2796.8	1259.3	993.3
(T)+EOM/CcCR	3003.8	1301.2	1033.7	2813.3	1274.8	1002.1
Exp.a				$2799.7 \pm 1.2$		
Exp. <sup>b</sup>						1021.26
Exp. <sup>c</sup>						$1000 \pm 20$
Exp. <sup>d</sup>					$1260 \pm 2$	

"Nauta, Guss, et al., 2004 (gas phase). <sup>63</sup> Merer and Travis, 1966; Hakuta, 1984 (gas phase). <sup>66,68</sup> Jacox and Milligan, 1969 (Argon). <sup>65</sup> Schmidt, Bacskay, et al., 1999 (gas phase). <sup>64</sup>

are similar in geometry to the ground-state configuration. However, more investigation is needed and will be carried out in future work.

The  $\nu_3$  mode for (T)+EOM/CcCR at 1274.8 cm<sup>-1</sup> agrees excellently with the Argon matrix data of Jacox and Milligan, 65 with only 2 cm<sup>-1</sup> difference between the two. However, the gas-phase data of Schmidt *et al.* 64 places the frequency higher at 1021.3 cm<sup>-1</sup>. Table 6 contains the geometric parameters and

Table 6. Ã ¹A" HCF Geometry and Rotational Frequencies

		(T)+EOM		
	units	Avtz	CcCR	
$R_0(H-C)$	Å	1.112	1.109	
$R_0(C-F)$	Å	1.310	1.302	
$\angle 0(H-C-F)$	Å	125.181	125.369	
$A_0$	MHz	25.714	26.044	
$B_0$	MHz	1.147	1.160	
$C_0$	MHz	1.093	1.106	
$A_1$	MHz	24.136	24.483	
$B_1$	MHz	1.145	1.158	
$C_1$	MHz	1.088	1.101	
$A_2$	MHz	25.634	25.972	
$B_2$	MHz	1.134	1.148	
$C_2$	MHz	1.082	1.095	
$A_3$	MHz	28.231	28.624	
$B_3$	MHz	1.149	1.162	
$C_3$	MHz	1.088	1.101	

rotational frequencies for HCF, which shows no marked discrepancy between the two levels of (T)+EOM. Ground-state frequencies and geometries are given in Tables S7 and S8. The gas-phase experiment places the  $\tilde{A}^1A'' \leftarrow \tilde{X}^1A'$  transition at 17,277 cm<sup>-1</sup>. <sup>63,64,66,67</sup> The calculated AEE for (T)+EOM/ CcCR is 17,230 cm<sup>-1</sup>, a difference of less than a mere 50 cm<sup>-1</sup>.

The  $\tilde{\rm A}$   $^1A''$  HNO data given in Table 7 show a moderate agreement with the experiment. The  $\nu_2$  mode for (T)+EOM/ avtz at 1419.7 cm<sup>-1</sup> agrees closely with the experimental values of Dalby at 1420.8 cm<sup>-169</sup> and Robinson and McCarty at 1422 cm<sup>-1,70,71</sup> However, the calculated (T)+EOM/CcCR frequency for this mode is higher at 1459.5 cm<sup>-1</sup>. EOM-CCSD calculations with aug-cc-pVXZ (X = T,Q,5) are given in Table 7, and these show a trend of increasing frequency with increasing basis set quality for  $\nu_2$ . This is also observed with the increase in basis set quality from (T)+EOM/avtz to (T)+EOM/CcCR. Therefore, the divergence from the experiment seen with the latter here may be a result of potential issues with EOM, coupled cluster theories, or possibly

experimental error, rather than fault specifically with the (T)+EOM approach. Both (T)+EOM methods agree reasonably well for  $\nu_3$ , which Dalby places at 981.2 cm $^{-1}$  and Robinson and McCarty determine to be 982 cm $^{-1}$ . The frequency for this mode is calculated to 987.4 cm $^{-1}$  for (T)+EOM/CcCR and 974.0 cm $^{-1}$  for (T)+EOM/avtz. Neither method agrees well with Bancroft et~al.'s assignment for  $\nu_1$  at 2854.2 cm $^{-1}$ , with both placing the mode approximately 40 cm $^{-1}$  higher. The calculated AEE for  $\tilde{\rm A}~^1A''$  HNO is 13,266 cm $^{-1}$  compared to the gas-phase experiment value of 13,154 cm $^{-1}$ . Performance of the (T)+EOM QFFs is not as strong for HNO as HCF, but this may have to do with the known anharmonicity issues of the anharmonic H–N stretch previously reported.

Table 8 shows a reasonably large difference between the two (T)+EOM methods for  $\angle$ (H-N-O), which is 115.268° for

Table 8. Ã <sup>1</sup>A" HNO Geometry and Rotational Frequencies

		(T)+EOM	
	units	avtz	CcCR
$R_0(H-N)$	Å	1.055	1.052
$R_0(N-O)$	Å	1.247	1.237
∠0(H-N-O)	Å	115.268	116.068
$A_0$	MHz	17.631	22.450
$B_0$	MHz	0.926	1.331
$C_0$	MHz	0.877	1.250
$A_1$	MHz	16.960	21.045
$B_1$	MHz	0.926	1.334
$C_1$	MHz	0.876	1.249
$A_2$	MHz	18.071	22.114
$B_2$	MHz	0.922	1.317
$C_2$	MHz	0.870	1.237
$A_3$	MHz	17.592	24.205
$B_3$	MHz	0.913	1.334
$C_3$	MHz	0.865	1.244

(T)+EOM/avtz and 116.068° for (T)+EOM/CcCR. This difference is likely due to contribution from core correlation in (T)+EOM/CcCR and may contribute to (T)+EOM/CcCR's poorer comparison with the experiment relative to (T)+EOM/avtz, as the shift in geometry may affect the CCSD(T) ground-state energy term in the (T)+EOM energy. Ground-state calculations for this molecule are given in Tables S10 and S11 and show good agreement between the ground-state QFFs and experiment.

Table 7. Ã ¹A" HNO Harmonic and Anharmonic Vibrational Frequencies

	$\omega_1$	$\omega_2$	$\omega_3$	$ u_1 $	$ u_2$	$ u_3$
description	H-N str.	N-O str.	H-N-O bend	H-N str.	N-O str.	H-N-O bend
(T)+EOM/avtz	3140.5	1458.8	990.2	2887.6	1419.7	974.0
(T)+EOM/CcCR	3154.1	1497.5	1006.4	2900.8	1459.5	987.4
EOM-CCSD/avtz	3207.0	1560.6	1020.6	2966.9	1527.3	1004.2
EOM-CCSD/avqz	3216.9	1582.7	1029.2	2975.5	1549.7	1012.0
EOM-CCSD/av5z	3218.0	1587.4	1031.8	2975.8	1554.5	1010.7
Exp. <sup>a</sup>				2854.2		
Exp. <sup>b</sup>					1420.77	981.18
Exp. <sup>c</sup>					1422	982

<sup>&</sup>lt;sup>a</sup>Bancroft, Hollas, et al., 1962 (gas). <sup>72</sup> <sup>b</sup>Dalby, 1958 (gas). <sup>69</sup> <sup>c</sup>Robinson and McCarty, 1958; Robinson and McCarty, 1958, 2 (Argon). <sup>70,71</sup>

## 4. CONCLUSIONS

Overall, (T)+EOM QFFs potentially offer a robust and costeffective approach for examining the rovibrational properties of electronically excited states. The method depends entirely on CCSD(T) and EOM-CCSD pieces, which are widely available in quantum chemistry packages for both closed and open shell systems and are often not prohibitively expensive. This means (T)+EOM could potentially be applied to a wide range of molecules.

(T)+EOM/CcCR and (T)+EOM/avtz compares favorably with established benchmark ground-state QFFs for HOO and HNF and agrees reasonably with the experiment for all four test cases. Results are particularly good for HOO and HNF, the latter of which shows a MAE of 7.5 cm<sup>-1</sup> between (T)+EOM/CcCR and F12-TZ. HCF and HNO match closer to the experiment for (T)+EOM/avtz than (T)+EOM/CcCR does. However, EOM-CCSD calculations show that this may not be unique to (T)+EOM and could possibly be the result of experimental error. This merits further investigation of the (T)+EOM method and how it fares relative to other excited state QFFs, such as QFFs based on EOM-CC3. The method may not perform as strongly with electronically excited states dominated by double or higher excitations or ones that have geometries significantly different than the ground-state configuration since those were not analyzed in the present work based on known issues with EOM-CCSD.8 It also remains to be seen how the method fares for molecules with more complicated symmetry internal coordinate schemes, but that will be dealt in future work.

# ASSOCIATED CONTENT

# **Solution** Supporting Information

The Supporting Information is available free of charge at https://pubs.acs.org/doi/10.1021/acs.jctc.1c00307.

Vibrational frequencies, geometric parameters, and rotational constants for electronic ground states of HOO, HNF, HCF and HNO, as well as scans for the electronically excited states of HOO and HNF, and force constants provided for the electronically excited states of the molecules examined (PDF)

# AUTHOR INFORMATION

## **Corresponding Author**

Ryan C. Fortenberry — Department of Chemistry & Biochemistry, University of Mississippi, University, Mississippi 38677-1848, United States; orcid.org/0000-0003-4716-8225; Email: r410@olemiss.edu

# Author

Megan C. Davis – Department of Chemistry & Biochemistry, University of Mississippi, University, Mississippi 38677-1848, United States; oorcid.org/0000-0002-4038-8615

Complete contact information is available at: https://pubs.acs.org/10.1021/acs.jctc.1c00307

#### Notes

The authors declare no competing financial interest.

# ■ ACKNOWLEDGMENTS

Funding is acknowledged from NSF grant OIA-1757220, NASA grant NNX17AH15G, and start-up funds provided by the University of Mississippi. Additionally, the computing

resources were provided in part by the Mississippi Center for Supercomputing Research funded with contributions from NSF grant CHE-1757888.

### REFERENCES

- (1) Dreuw, A.; Head-Gordon, M. Single-Reference ab initio Methods for the Calculation of Excited States of Large Molecules. *Chem. Rev.* **2005**, *105*, 4009–4037.
- (2) González, L.; Escudero, D.; Serrano-Andrés, L. Progress and Challenges in the Calculation of Electronic Excited States. *ChemPhysChem* **2012**, *13*, 28–51.
- (3) Fortenberry, R. C. Quantum Astrochemical Spectroscopy. *Int. J. Quant. Chem.* **2017**, *117*, 81–91.
- (4) Raghavachari, K.; Trucks, G. W.; Pople, J. A.; Head-Gordon, M. A Fifth-Order Perturbation Comparison of Electron Correlation Theories. *Chem. Phys. Lett.* **1989**, *157*, 479–483.
- (5) Shavitt, I.; Bartlett, R. J. Many-Body Methods in Chemistry and Physics: MBPT and Coupled-Cluster Theory; Cambridge University Press: Cambridge, 2009.
- (6) Crawford, T. D.; Schaefer, H. F., III Reviews in Computational Chemistry; Lipkowitz, K. B., Boyd, D. B., Eds.; Wiley: New York, 2000; Vol. 14, pp 33–136.
- (7) Stanton, J. F.; Bartlett, R. J. The Equation of Motion Coupled-Cluster Method A Systematic Biorthogonal Approach to Molecular Excitation Energies, Transition-Probabilities, and Excited-State Properties. J. Chem. Phys. 1993, 98, 7029—7039.
- (8) Fortenberry, R. C.; King, R. A.; Stanton, J. F.; Crawford, T. D. A Benchmark Study of the Vertical Electronic Spectra of the Linear Chain Radicals C<sub>2</sub>H and C<sub>4</sub>H. *J. Chem. Phys.* **2010**, *132*, 144303.
- (9) Runge, E.; Gross, E. K. U. Density-Functional Theory for Time-Dependent Systems. *Phys. Rev. Lett.* **1984**, *52*, 997–1000.
- (10) Ghosh, S.; Verma, P.; Cramer, C. J.; Gagliardi, L.; Truhlar, D. G. Combining Wave Function Methods with Density Functional Theory for Excited States. *Chem. Rev.* **2018**, *118*, 7249–7292.
- (11) Matthews, D. A.; Stanton, J. F. A New Approach to Approximate Equation-of-Motion Coupled Cluster with Triple Excitations. *J. Chem. Phys.* **2016**, *145*, 124102.
- (12) Tajti, A.; Stanton, J. F.; Matthews, D. A.; Szalay, P. G. Accuracy of Coupled Cluster Excited State Potential Energy Surfaces. *J. Chem. Theory Comput.* **2018**, *14*, 5859–5869.
- (13) Loos, P.-F.; Scemama, A.; Jacquemin, D. The Quest for Highly Accurate Excitation Energies: A Computational Perspective. *J. Phys. Chem. Lett.* **2020**, *11*, 2374–2383.
- (14) Watson, T. J.; Lotrich, V. F.; Szalay, P. G.; Perera, A.; Bartlett, R. J. Benchmarking for Perturbative Triple-Excitations in EE-EOM-CC Methods. *J. Phys. Chem. A* **2013**, *117*, 2569–2579.
- (15) Rishi, V.; Perera, A.; Nooijen, M.; Bartlett, R. J. Excited States from Modified Coupled Cluster Methods: Are They Any Better Than EOM CCSD? *J. Chem. Phys.* **2017**, *146*, 144104.
- (16) Krylov, A. Reviews in Computational Chemistry; Wiley, 2017; Chapter 4, pp 151-224.
- (17) Koch, H.; Christiansen, O.; Jørgensen, P.; de Meràs, A. M. S.; Helgaker, T. The CC3 Model: An Iterative Coupled Cluster Approach including Connected Triples. *J. Chem. Phys.* **1997**, *106*, 1808–1818
- (18) Smith, C. E.; King, R. A.; Crawford, T. D. Coupled cluster methods including triple excitations for excited states of radicals. *J. Chem. Phys.* **2005**, 122, 054110.
- (19) Kowalski, K.; Piecuch, P. New Coupled-Cluster Methods with Singles, Doubles, and Noniterative Triples for High Accuracy Calculations of Excited Electronic States. *J. Chem. Phys.* **2004**, *120*, 1715–1738.
- (20) Watts, J. D.; Bartlett, R. J. Economical Triple Excitation Equation-of-Motion Coupled-Cluster Methods for Excitation Energies. *Chem. Phys. Lett.* **1995**, 233, 81–87.
- (21) Fortenberry, R. C.; Lee, T. J. Computational Vibrational Spectroscopy for the Detection of Molecules in Space. *Annu. Rep. Comput. Chem.* **2019**, *15*, 173–202.

- (22) Huang, X.; Taylor, P. R.; Lee, T. J. Highly Accurate Quartic Force Field, Vibrational Frequencies, and Spectroscopic Constants for Cyclic and Linear C<sub>3</sub>H<sub>3</sub><sup>+</sup>. *J. Phys. Chem. A* **2011**, *115*, 5005–5016.
- (23) Fortenberry, R. C.; Huang, X.; Francisco, J. S.; Crawford, T. D.; Lee, T. J. Quartic Force Field Predictions of the Fundamental Vibrational Frequencies and Spectroscopic Constants of the Cations HOCO<sup>+</sup> and DOCO<sup>+</sup>. *J. Chem. Phys.* **2012**, *136*, 234309.
- (24) Fortenberry, R. C.; Huang, X.; Francisco, J. S.; Crawford, T. D.; Lee, T. J. Fundamental Vibrational Frequencies and Spectroscopic Constants of HOCS<sup>+</sup>, HSCO<sup>+</sup>, and Isotopologues via Quartic Force Fields. *J. Phys. Chem. A* **2012**, *116*, 9582–9590.
- (25) Zhao, D.; Doney, K. D.; Linnartz, H. LABORATORY GAS-PHASE DETECTION OF THE CYCLOPROPENYL CATION (c-C 3 H 3 + ). Astrophys. J., Lett. 2014, 791, L28.
- (26) Morgan, W. J.; Fortenberry, R. C. Theoretical Rovibronic Treatment of the  $X \sim 2\Sigma +$  and  $A \sim 2\Pi$  States of  $C_2H$  &  $X \sim 1\Sigma +$  State of  $C_2H^-$  from Quartic Force Fields. J. Phys. Chem. A **2015**, 119, 7013–7025.
- (27) Theis, R. A.; Fortenberry, R. C. Potential Interstellar Noble Gas Molecules: ArOH<sup>+</sup> and NeOH<sup>+</sup> Rovibrational Analysis from Quantum Chemical Quartic Force Fields. *Mol. Astrophys.* **2016**, *2*, 18–24.
- (28) Bizzocchi, L.; Lattanzi, V.; Laas, J.; Spezzano, S.; Giuliano, B. M.; Prudenzano, D.; Endres, C.; Sipilä, O.; Caselli, P. Accurate Submillimetre Rest Frequencies for HOCO<sup>+</sup> and DOCO<sup>+</sup> Ions. *Astron. Astrophys.* **2017**, *602*, A34.
- (29) Kitchens, M. J. R.; Fortenberry, R. C. The rovibrational nature of closed-shell third-row triatomics: HOX and HXO, X = Si+, P, S+, and Cl. *Chem. Phys.* **2016**, *472*, 119–127.
- (30) Fortenberry, R. C.; Francisco, J. S. On the Detectability of the  $X\sim2A''$  HSS, HSO, and HOS Radicals in the Interstellar Medium. *Astrophys. J.* **2017**, 835, 243.
- (31) Fuente, A.; Goicoechea, J. R.; Pety, J.; Gal, R. L.; Martín-Doménech, R.; Gratier, P.; Guzmán, V.; Roueff, E.; Loison, J. C.; Caro, G. M. M.; Wakelam, V.; Gerin, M.; Riviere-Marichalar, P.; Vidal, T. First Detection of Interstellar S<sub>2</sub>H. *Astrophys. J., Lett.* **2017**, 851, L49.
- (32) Wagner, J. P.; McDonald, D. C., II; Duncan, M. A. An Argon—Oxygen Covalent Bond in the ArOH<sup>+</sup> Molecular Ion. *Angew. Chem., Int. Ed.* **2018**, *57*, 5081–5085.
- (33) Gardner, M. B.; Westbrook, B. R.; Fortenberry, R. C.; Lee, T. J. Highly-Accurate Quartic Force Fields for the Prediction of Anharmonic Rotational Constants and Fundamental Vibrational Frequencies. *Spectrochim. Acta, Part A* **2021**, 248, 119184.
- (34) Fortenberry, R. C.; Trabelsi, T.; Francisco, J. S. Hydrogen Sulfide as a Scavenger of Sulfur Atomic Cation. *J. Phys. Chem. A* **2018**, 122, 4983–4987.
- (35) Morgan, W. J.; Fortenberry, R. C. Quartic Force Fields for Excited Electronic States: Rovibronic Reference Data for the 1 <sup>2</sup>A' and 1 <sup>2</sup>A'' States of the Isoformyl Radical, HOC. Spectrochim. Acta, Part A 2015, 135, 965–972.
- (36) Allen, W. D.; et al. INTDER 2005 Is a General Program Written by W. D. Allen and Coworkers, Which Performs Vibrational Analysis and Higher-Order Non-linear Transformations, 2005.
- (37) Gaw, J. F.; Willets, A.; Green, W. H.; Handy, N. C. Advances in Molecular Vibrations and Collision Dynamics; Bowman, J. M., Ratner, M. A., Eds.; JAI Press, Inc.: Greenwich, Connecticut, 1991; pp 170–185.
- (38) Mills, I. M. Molecular Spectroscopy—Modern Research; Rao, K. N., Mathews, C. W., Eds.; Academic Press: New York, 1972; pp 115–140
- (39) Watson, J. K. G. Vibrational Spectra and Structure; During, J. R., Ed.; Elsevier: Amsterdam, 1977; pp 1–89.
- (40) Papousek, D.; Aliev, M. R. Molecular Vibration-Rotation Spectra; Elsevier: Amsterdam, 1982.
- (41) Adler, T. B.; Knizia, G.; Werner, H.-J. A Simple and Efficient CCSD(T)-F12 Approximation. J. Chem. Phys. 2007, 127, 221106.

- (42) Peterson, K. A.; Adler, T. B.; Werner, H.-J. Systematically Convergent Basis Sets for Explicitly Correlated Wavefunctions: The Atoms H, He, B-Ne, and Al-Ar. *J. Chem. Phys.* **2008**, *128*, 084102.
- (43) Yousaf, K. E.; Peterson, K. A. Optimized Auxiliary Basis Sets for Explicitly Correlated Methods. *J. Chem. Phys.* **2008**, *129*, 184108.
- (44) Knizia, G.; Adler, T. B.; Werner, H.-J. Simplified CCSD(T)-F12 Methods: Theory and Benchmarks. *J. Chem. Phys.* **2009**, *130*, 054104.
- (45) Martin, J. M. L.; Taylor, P. R. Basis Set Convergence for Geometry and Harmonic Frequencies. Are h Functions Enough? *Chem. Phys. Lett.* **1994**, 225, 473–479.
- (46) Martin, J. M. L.; Lee, T. J. The atomization energy and proton affinity of NH3. An ab initio calibration study. *Chem. Phys. Lett.* **1996**, 258, 136–143.
- (47) Douglas, M.; Kroll, N. Quantum Electrodynamical Corrections to the Fine Structure of Helium. *Ann. Phys.* **1974**, 82, 89–155.
- (48) Fortenberry, R. C.; Huang, X.; Francisco, J. S.; Crawford, T. D.; Lee, T. J. The trans-HOCO radical: Quartic force fields, vibrational frequencies, and spectroscopic constants. *J. Chem. Phys.* **2011**, *135*, 134301.
- (49) Werner, H.-J.; Knowles, P. J.; Knizia, G.; Manby, F. R.; Schütz, M.; Celani, P.; Györffy, W.; Kats, D.; Korona, T.; Lindh, R.; Mitrushenkov, A.; Rauhut, G.; Shamasundar, K. R.; Adler, T. B.; Amos, R. D.; Bernhardsson, A.; Berning, A.; Cooper, D. L.; Deegan, M. J. O.; Dobbyn, A. J.; Eckert, F.; Goll, E.; Hampel, C.; Hesselmann, A.; Hetzer, G.; Hrenar, T.; Jansen, G.; Köppl, C.; Liu, Y.; Lloyd, A. W.; Mata, R. A.; May, A. J.; McNicholas, S. J.; Meyer, W.; Mura, M. E.; Nicklass, A.; O'Neill, D. P.; Palmieri, P.; Peng, D.; Pflüger, K.; Pitzer, R.; Reiher, M.; Shiozaki, T.; Stoll, H.; Stone, A. J.; Tarroni, R.; Thorsteinsson, T.; Wang, M. MOLPRO, Version 2015.1, a Package of ab Initio Programs, 2015; see http://www.molpro.net.
- (50) Aprà, E.; Bylaska, E. J.; de Jong, W. A.; Govind, N.; Kowalski, K.; Straatsma, T. P.; Valiev, M.; van Dam, H. J. J.; Alexeev, Y.; Anchell, J.; Anisimov, V.; Aquino, F. W.; Atta-Fynn, R.; Autschbach, J.; Bauman, N. P.; Becca, J. C.; Bernholdt, D. E.; Bhaskaran-Nair, K.; Bogatko, S.; Borowski, P.; Boschen, J.; Brabec, J.; Bruner, A.; Cauët, E.; Chen, Y.; Chuev, G. N.; Cramer, C. J.; Daily, J.; Deegan, M. J. O.; Dunning, T. H.; Dupuis, M.; Dyall, K. G.; Fann, G. I.; Fischer, S. A.; Fonari, A.; Früchtl, H.; Gagliardi, L.; Garza, J.; Gawande, N.; Ghosh, S.; Glaesemann, K.; Götz, A. W.; Hammond, J.; Helms, V.; Hermes, E. D.; Hirao, K.; Hirata, S.; Jacquelin, M.; Jensen, L.; Johnson, B. G.; Jónsson, H.; Kendall, R. A.; Klemm, M.; Kobayashi, R.; Konkov, V.; Krishnamoorthy, S.; Krishnan, M.; Lin, Z.; Lins, R. D.; Littlefield, R. J.; Logsdail, A. J.; Lopata, K.; Ma, W.; Marenich, A. V.; Martin del Campo, J.; Mejia-Rodriguez, D.; Moore, J. E.; Mullin, J. M.; Nakajima, T.; Nascimento, D. R.; Nichols, J. A.; Nichols, P. J.; Nieplocha, J.; dela Roza, A. O.; Palmer, B.; Panyala, A.; Pirojsirikul, T.; Peng, B.; Peverati, R.; Pittner, J.; Pollack, L.; Richard, R. M.; Sadayappan, P.; Schatz, G. C.; Shelton, W. A.; Silverstein, D. W.; Smith, D. M. A.; Soares, T. A.; Song, D.; Swart, M.; Taylor, H. L.; Thomas, G. S.; Tipparaju, V.; Truhlar, D. G.; Tsemekhman, K.; Van Voorhis, T.; Vázquez-Mayagoitia, Á.; Verma, P.; Villa, O.; Vishnu, A.; Vogiatzis, K. D.; Wang, D.; Weare, J. H.; Williamson, M. J.; Windus, T. L.; Woliński, K.; Wong, A. T.; Wu, Q.; Yang, C.; Yu, Q.; Zacharias, M.; Zhang, Z.; Zhao, Y.; Harrison, R. J. NWChem: Past, present, and future. J. Chem. Phys. 2020, 152, 184102.
- (51) Martin, J. M. L.; Taylor, P. R. Accurate ab Initio Quartic Force Field for trans-HNNH and Treatment of Resonance Polyads. *Spectrochim. Acta, Part A* **1997**, *53*, 1039–1050.
- (52) Hunziker, H. E.; Wendt, H. R. Electronic Absorption Spectra of Organic Peroxyl Radicals in the Near Infrared. *J. Chem. Phys.* **1976**, *64*, 3488–3490.
- (53) Becker, K. H.; Fink, E. H.; Leiss, A.; Schurath, U. A Study of the Near Infrared Emission Bands of the Hydroperoxyl Radical at Medium Resolution. *Chem. Phys. Lett.* **1978**, *54*, 191–196.
- (54) Fink, E. H.; Kruse, H.; Ramsay, D. A. Paper WF2, 42nd Symposium on Molecular Spectroscopy, 1987.

- (55) Holstein, K. J.; Fink, E. H.; Zabel, F. The  $\nu 3$  vibration of electronically excited HO2(A2A'). *J. Mol. Spectrosc.* **1983**, *99*, 231–234.
- (56) Woodman, C. M. The absorption spectrum of HNF in the region 3800-5000 Å. *I. Mol. Spectrosc.* 1970, 33, 311-344.
- (57) Jacox, M. E.; Milligan, D. E. Production and Reaction of Atomic Fluorine in Solids. Vibrational and Electronic Spectra of the Free Radical HNF. *J. Chem. Phys.* **1967**, *46*, 184–191.
- (58) Trabelsi, T.; Davis, M. C.; Fortenberry, R. C.; Francisco, J. S. Spectroscopic Investigation of [Al,N,C,O] Refractory Molecules. *J. Chem. Phys.* **2019**, *151*, 244303.
- (59) Bassett, M. K.; Fortenberry, R. C. Symmetry Breaking and Spectral Considerations of the Surprisingly Floppy  $c-C_3H$  Radical and the Related Dipole-Bound Excited State of  $c-C_3H^-$ . *J. Chem. Phys.* **2017**, *146*, 224303.
- (60) Agbaglo, D.; Lee, T. J.; Thackston, R.; Fortenberry, R. C. A Small Molecule with PAH Vibrational Properties and a Detectable Rotational Spectrum: c-(C)C<sub>3</sub>H<sub>2</sub>. Cyclopropenylidenyl Carbene. *Astrophys. J.* **2019**, *871*, 236.
- (61) Agoaglo, D.; Fortenberry, R. C. The performance of explicitly correlated methods for the computation of anharmonic vibrational frequencies. *Int. J. Quantum Chem.* **2019**, *119*, No. e25899.
- (62) Agbaglo, D.; Fortenberry, R. C. The Performance of Explicitly Correlated Wavefunctions [CCSD(T)-F12b] in the Computation of Anharmonic Vibrational Frequencies. *Chem. Phys. Lett.* **2019**, 734, 136720
- (63) Nauta, K.; Guss, J. S.; Owens, N. L.; Kable, S. H. Reassignment of the CH Stretching Frequency of CHF in the A Electronic State. *J. Chem. Phys.* **2004**, *120*, 3517–3518.
- (64) Schmidt, T. W.; Bacskay, G. B.; Kable, S. H. Characterization of the  $\tilde{A}(1A'')$  state of HCF by laser induced fluorescence spectroscopy. *J. Chem. Phys.* **1999**, *110*, 11277–11285.
- (65) Jacox, M. E.; Milligan, D. E. Matrix-Isolation Study of the Vacuum-Ultraviolet Photolysis of Methyl Fluoride. The Infrared Spectra of the Free Radicals CF, HCF, and H2CF. *J. Chem. Phys.* **1969**, *50*, 3252–3262.
- (66) Merer, A. J.; Travis, D. N. Rotational Analysis of Bands of the HCF Molecule. *Can. J. Phys.* **1966**, *44*, 1541–1550.
- (67) Fan, H.; Mukarakate, C.; Deselnicu, M.; Tao, C.; Reid, S. A. Dispersed Fluorescence Spectroscopy of Jet-Cooled HCF and DCF: Vibrational Structure of the  $\tilde{X}$  <sup>1</sup>A' State. *J. Chem. Phys.* **2005**, *123*, 014314.
- (68) Hakuta, K. Vibration-rotation spectrum of HCF () by laser-induced fluorescence. J. Mol. Spectrosc. 1984, 106, 56-63.
- (69) Dalby, F. W. The Spectrum and Structure of the HNO Molecule. Can. J. Phys. 1958, 36, 1336–1371.
- (70) Robinson, G. W.; McCarty, M. Electronic Spectra of Free Radicals at 4°K-HNO, NH, and OH. J. Chem. Phys. 1958, 28, 350.
- (71) Robinson, G. W.; McCarty, M., Jr Radical Spectra at Liquid Helium Temperatures. Can. J. Phys. 1958, 36, 1590-1591.
- (72) Bancroft, J. L.; Hollas, J. M.; Ramsay, D. A. The Absorption Spectra of HNO and DNO. Can. J. Phys. 1962, 40, 322-347.
- (73) Dateo, C. E.; Lee, T. J.; Schwenke, D. W. An Accurate Quartic Force-Field and Vibrational Frequencies for HNO and DNO. *J. Chem. Phys.* **1994**, *101*, 5853–5859.